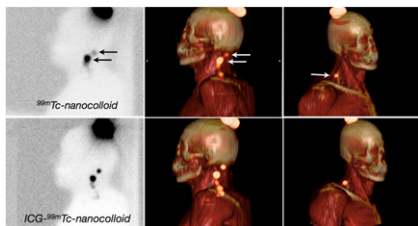


PET/CT staging in NSCLC: Gregory and colleagues detail the effect on management and prognostic value of ^{18}F -FDG PET/CT staging in patients with non-small cell lung cancer being considered for potentially curative therapies. **Page 1007**

PET and RCTs: Scheibler and colleagues provide an overview of the numbers, clinical topics, design, and quality of current randomized controlled trials evaluating PET and PET/CT. **Page 1016**

Hybrid sentinel node mapping: Buckle and colleagues describe intraprostatic injection of indocyanine green- $^{99\text{m}}\text{Tc}$ -nanocolloid to enable both preoperative sentinel node identification and intraoperative visualization. **Page 1026**

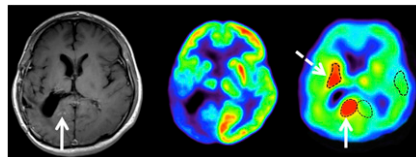
Hybrid sentinel node tracer validation: Brouwer and colleagues compare the lymphoscintigraphic drainage patterns of fluorescent indocyanine green and $^{99\text{m}}\text{Tc}$ -nanocolloid with the drainage pattern of $^{99\text{m}}\text{Tc}$ -nanocolloid alone in patients with melanoma or penile carcinoma. **Page 1034**



Noise considerations in PET quantification: Lodge and colleagues measure aspects of bias and reproducibility associated with maximum and peak ^{18}F -FDG PET SUVs using clinical treatment monitoring data to provide realistic noise contexts. **Page 1041**

Response assessment with ^{18}F -FET PET: Galldiks and colleagues explore the predictive value of ^{18}F -FET PET in determining treatment response in glioblastoma and compare results with those obtained using MRI. **Page 1048**

Recurrent gliomas and ^{11}C -AMT PET: Alkonyi and colleagues evaluate the utility of α - ^{11}C -methyl-L-tryptophan PET supplemented by tracer kinetic analysis for distinguishing recurrent gliomas from radiation injury. **Page 1058**



^{18}F -FE-PE2I in humans: Sasaki and colleagues look at quantification of dopamine transporters in human volunteers, with a new PET radioligand that in animal studies has shown fast kinetics and low production of radiometabolites. . . . **Page 1065**

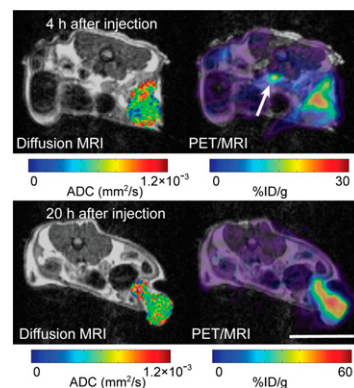
PET and MRI in SCA17: Brockmann and colleagues assess functional and morphologic imaging characteristics to identify evidence of neurodegeneration in early stages of spinocerebellar ataxia type 17, a rare autosomal disorder. . . . **Page 1074**

Calcium score and preoperative risk: Ghadri and colleagues research the added value of coronary artery calcium score as an adjunct to SPECT myocardial perfusion imaging for cardiac risk stratification before noncardiac surgery. **Page 1081**

^{123}I -FP-CIT SPECT SERT measurement: Koopman and colleagues examine the extrastriatal binding of this agent commonly used to assess striatal dopamine transporter binding to determine optimal time points for SPECT measurement of serotonin transporter binding. . . . **Page 1087**

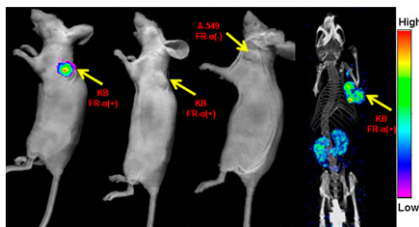
Imaging multiple myeloma: Walker and colleagues present an educational overview of imaging of multiple myeloma and related plasma cell dyscrasias, including the role of advanced imaging in diagnosis, staging, and restaging. **Page 1091**

Quantitative in vivo PET/MR: Ng and colleagues describe and evaluate the ability of a first-generation, small-animal MRI-compatible PET scanner to accurately depict heterogeneous patterns of radiotracer uptake in tumors. **Page 1102**



^{18}F -Affibody for EGFR imaging: Miao and colleagues report on the successful site-specific labeling of an Affibody analog for PET imaging of epidermal growth factor receptors and review the potential for translation to clinical use. . . . **Page 1110**

ER/PR PET and endocrine therapy: Fowler and colleagues use estrogen- and progesterin-based radiopharmaceuticals to image estrogen receptor- α and progesterone receptor in mouse mammary tumors during hormonal therapy to determine whether changes can predict therapeutic response. **Page 1119**



PARP-1 and ^{131}I -MIBG/topotecan: McCluskey and colleagues report on the potential of polyadenosine diphosphate ribose polymerase inhibition as a means to enhance targeted therapy with ^{131}I -MIBG and the topoisomerase I inhibitor topotecan. **Page 1146**

Folate receptor- α -specific targeting ligand: Vaitilingam and colleagues detail the development of a reduced and alkylated form of folic acid for use in a targeting ligand to selectively deliver attached imaging and therapeutic agents to tumor cells. **Page 1127**

Growth dynamics of glioblastomas: Viel and colleagues use multimodal small animal PET and MRI to analyze the growth of angiogenesis-dependent and -independent experimental glioblastomas at various stages. **Page 1135**

No-carrier-added ^{131}I -MIBG: Matthey and colleagues establish the maximum tolerated dose of no-carrier-added ^{131}I -MIBG in patients with resistant neuroblastoma and assess tumor and organ dosimetry and overall response. **Page 1155**

ON THE COVER

Estrogen receptor- α and progesterone receptor are expressed in most human breast cancers and are important predictive factors for directing therapy. A preclinical study in this issue of *JNM* demonstrates that imaging baseline tumoral ^{18}F -FES uptake and initial changes in ^{18}F -FFNP uptake is a potentially useful, noninvasive strategy to identify responders and nonresponders to endocrine therapy at an early stage.

See page 1121.

